

A Phyllopod-Mediated Feedback Loop Promotes Intestinal Stem Cell Enteroendocrine Commitment in *Drosophila*

Chang Yin^{1,2} and Rongwen Xi^{1,2,3,*}¹Graduate School of Peking Union Medical College, Chinese Academy of Medical Sciences and Peking Union Medical College, Beijing 100730, China²National Institute of Biological Sciences, No. 7 Science Park Road, Zhongguancun Life Science Park, Beijing 102206, China³Institute for Regenerative Medicine, Shanghai East Hospital, School of Life Sciences and Technology, Tongji University, Shanghai 200092, China*Correspondence: xirongwen@nibs.ac.cn<https://doi.org/10.1016/j.stemcr.2017.11.014>

SUMMARY

The intestinal epithelium in the *Drosophila* midgut is maintained by intestinal stem cells (ISCs), which are capable of generating both enterocytes and enteroendocrine cells (EEs) via alternative cell fate specification. Activation of Delta-Notch signaling directs ISCs for enterocyte generation, but how EEs are generated from ISCs remains poorly understood. Here, we identified Phyllopod (Phyl) as a key regulator that drives EE generation from ISCs. Phyl, which is normally suppressed by Notch, functions as an adaptor protein that bridges Tramtrack 69 (Ttk69) and E3 ubiquitin ligase Sina for degradation. Degradation of Ttk69 allows the activation of the Achaete-Scute Complex (AS-C)-Pros regulatory axis, which promotes EE specification. Interestingly, expression of AS-C genes in turn further induces Phyl expression, thereby establishing a positive feedback loop for continuous EE fate specification and commitment. This positive feedback circuit-driven regulatory mechanism could represent a common strategy for reliable and irreversible cell fate determination from progenitor cells.

INTRODUCTION

A fundamental question in developmental biology is how cells acquire their fates. Specification of cell fate occurs during animal development, as well as in renewable adult tissues in which new cells are constantly generated by resident stem cells. Although transcription factors are commonly involved in determining cellular identities (Graf and Enver, 2009; Zernicka-Goetz et al., 2009), how their expression and activity are regulated to control progressive and reliable cell fate determination is in general poorly understood and requires detailed analysis in each individual developmental context.

Intestinal epithelium in *Drosophila* midgut provides a relatively simple and genetically tractable experimental system for studies of cell fate specification from stem cells (Biteau et al., 2011; Jiang and Edgar, 2011). Intestinal stem cells (ISCs) in *Drosophila* posterior midgut periodically produce committed progenitor cells termed enteroblasts (EBs) that differentiate further into either absorptive enterocytes (ECs) or secretory enteroendocrine cells (EEs) (Michelli and Perrimon, 2006; Ohlstein and Spradling, 2006). The exit of ISC self-renewal and control of the binary fate decision of EBs is primarily controlled by Delta (Dl)-Notch signaling (Ohlstein and Spradling, 2007; Perdigoto et al., 2011). EBs with high Notch activation will adopt an EC fate, whereas EBs with low Notch activity will adopt an EE fate (Ohlstein and Spradling, 2007). Notch activation induces expression of the genes of the enhancer of split complex (E(spl)-C), which functions to promote ISC differentiation by antagonizing the bHLH transcription

factor Daughterless (Bardin et al., 2010). A number of genes or pathways have been implicated in regulating EE specification, including the transcriptional repressor Tramtrack 69 (Ttk69) (Wang et al., 2015), the *achaete-scute* complex (AS-C) genes (Amcheslavsky et al., 2014; Bardin et al., 2010) that encode several basic-helix-loop-helix (bHLH) transcriptional factors, and the EE-determination transcription factor Prospero (Pros) (Biteau and Jasper, 2014; Wang et al., 2015; Zeng and Hou, 2015), among others (Beebe et al., 2010; Biteau and Jasper, 2014; Jiang et al., 2009; Kapuria et al., 2012; Lin et al., 2010; Quan et al., 2013). We previously presented evidence to support the essential role of a Ttk69-AS-C-Pros regulatory axis that controls EE specification from ISCs. AS-C gene expression is normally repressed by Ttk69, and a Ttk69-null mutation forced all progenitor cells to adopt an EE fate. While it is thus clear that the regulation of AS-C and its attendant activation of Pros by Ttk69 controls EE specification, it remains unclear how Ttk69 is itself regulated (Wang et al., 2015).

In addition to recent work showing the role of Ttk in EE specification in the midgut, decades of studies have demonstrated that Ttk regulates cell fate specification in the development of other organs such as the eye and external sensory organs (Badenhorst, 2001; Badenhorst et al., 2002; Giesen et al., 1997; Guo et al., 1995; Li et al., 1997; Okabe et al., 2001; Tang et al., 1997; Xiong and Montell, 1993). Post-translational modification of Ttk has been shown to promote R7 photoreceptor and sensory organ precursor (SOP) specification: the E3 ubiquitin ligase Seven in absentia (Sina) and an adaptor protein Phyllopod





(Phyl) that ubiquitinate Ttk, which is subsequently degraded by the proteasome (Li et al., 1997, 2002; Pi et al., 2001; Tang et al., 1997). Here, we investigated the function of *sina* and *phyl* in the adult *Drosophila* midgut, and this led us to reveal a positive feedback loop that drives EE commitment from ISCs.

RESULTS

sina and *phyl* Are Both Required for EE Specification in the Adult *Drosophila* Midgut

To determine whether *sina* has a role in the ISC lineages in the adult midgut, we used the MARCM system to generate *sina* homozygous mutant ISC clones in heterozygous animals by induced mitotic recombination, and then analyzed the cell composition of GFP-marked clones originated from ISCs 1–2 weeks after clone induction (ACI) (Lee and Luo, 1999; Lin et al., 2008; Wang et al., 2015; Xu et al., 2011). Normally, during progenitor cell differentiation, about 10%–20% of EBs adopt the EE fate; the rest of the EBs adopt the EC fate. As a consequence, EE cells only represent a small fraction of ISC progeny in the midgut epithelium (Biteau and Jasper, 2014; Ohlstein and Spradling, 2007). Quantitative analysis of wild-type ISC clones at day 10 ACI revealed that EEs, which can be specifically identified using Pros as a marker, constituted approximately 6%–8% of the total cell population within the clones. In contrast, virtually no Pros-expressing cells could be detected in the GFP-marked *sina*² mutant clones (Figures 1A, 1B, and 1C). The *sina*² mutant allele encodes a truncated protein that lacks 105 amino acids of the C terminus of the Sina protein (Carthew and Rubin, 1990). GFP-marked clones of *sina*³, another loss-of-function allele of *sina*, exhibited an identical EE loss phenotype to that of *sina*² mutant clones (Figures S1A and S1B). We also stained these *sina*² mutant clones with *Drosophila* Tachykinin (dTK), a neuropeptide that is secreted by EEs. Virtually no dTK⁺ cells could be found in *sina*² mutant clones (Figure S1C). It is noteworthy that the size (cell number) of the clones was largely comparable between wild-type and *sina* mutant ISC clones, indicating that loss of *sina* does not affect ISC proliferation. Staining with antibodies against Pdm1, an EC marker, revealed that ECs were properly differentiated in *sina* mutant clones (Figure 1D). Taken together, these observations suggest that *sina* is specifically required for EE specification from ISCs.

Previous studies in *Drosophila* eye and external sensory organs have demonstrated that Phyl is an essential adaptor protein that bridges Sina and Ttk to enable Ttk polyubiquitination and degradation. Direct interaction between Sina and Ttk is rather weak, but the presence of Phyl allows the formation of a strong Sina-Phyl-Ttk protein

complex for subsequent protein modification and degradation, which is essential for proper photoreceptor differentiation (Li et al., 2002; Ou et al., 2003). To explore the function of *phyl* in EE fate specification, we generated GFP-marked MARCM clones homozygous for the *phyl* (*phyl*²³⁶⁶) mutant allele. Strikingly, at day 10 ACI, when the wild-type ISC clones had typically grown into patches of 10–30 cells comprising both ISCs and their derived progeny (polyploid ECs and diploid EEs) (Figure S2A), the *phyl* mutant ISC clones comprised only 1–3 cells (Figures 1E and 1F). Clones homozygous for the *phyl*²²⁴⁵ mutant allele, a genetic null, showed a similar growth defect (Figure S2C). The growth retardation of these mutant clones persisted over time; even at 3 weeks ACI, they still had only 1–3 cells (Figure S2B). Some cells of the mutant clones developed into large polyploid cells. Co-staining with the ISC marker D1 and the EE marker Pros revealed that some *phyl* mutant cells were positive for D1 (Figure 1E) and that none of the mutant clones (>500 clones examined) contained any Pros⁺ cells (Figure 1F). Staining with antibodies against phosphor-histone H3 (PH3) showed that none of the mutant clones (>300 clones examined) contained any mitotic cells, although PH3⁺ cells were present in wild-type clones and in the wild-type cells surrounding the mutant clones (Figures S2D and S2E). We also generated MARCM clones with *phyl*-RNAi expression, these clones were also devoid of EEs, and their clone sizes were also smaller than the wild-type clones, but this size phenotype was much milder than the *phyl* mutant clones, and many properly differentiated ECs were found in each clone (Figure S3). Because RNAi often reduces gene products but does not eliminate them, the presence of large EE-less clones suggests that the EE specification function of *phyl* is more sensitive to the gene dosage than the ISC proliferation function of *phyl*. Collectively, these results demonstrate that the loss of *phyl* causes decreased proliferation of ISCs and failed EE differentiation without affecting EC differentiation.

To further evaluate the role of *phyl* in regulating EE specification from ISCs, we used a GAL4-UAS binary expression system to knock down *phyl* expression (Brand and Perrimon, 1993). *esg-GAL4* was used to drive the ISC- and EB-specific expression of RNAi targeting *phyl* in female *esg-Gal4,UAS-GFP; UAS-phyl-RNAi (esg>phyl-RNAi)* flies. While Pros⁺ EEs were scattered throughout wild-type intestinal epithelia (Figure 1G), the epithelia of *esg>phyl-RNAi* midguts were completely devoid of Pros⁺ cells (Figures 1H and 1I). There was no apparent difference in the *esg>GFP*⁺ cell populations between wild-type and *esg>phyl-RNAi* midguts (Figures 1G–1J). These results further support the notion that *phyl* is required for EE specification from ISCs. Therefore, similar to *sina*, *phyl* is indispensable for EE specification in the midgut

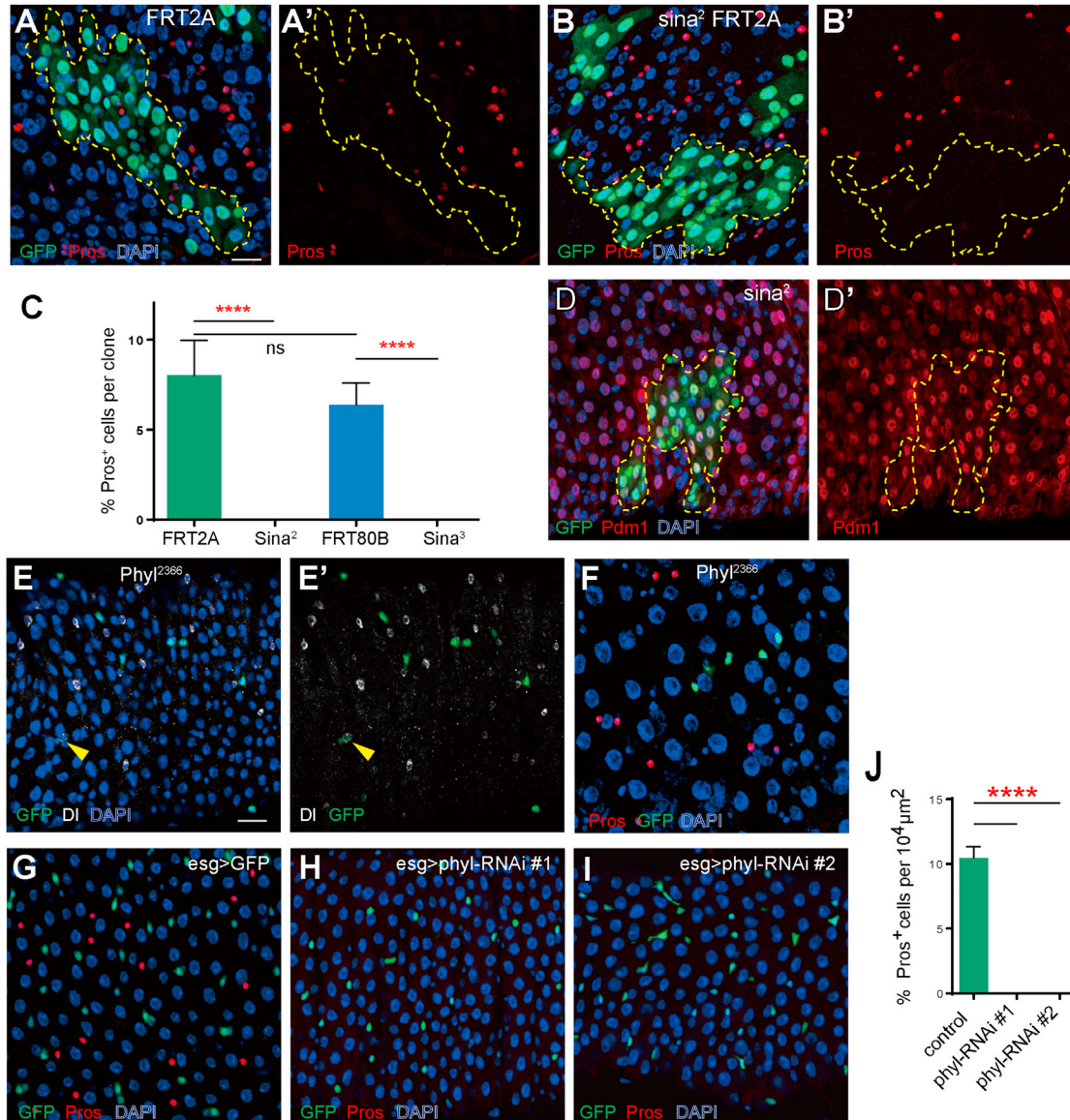


Figure 1. *sina* and *phyl* Are both Required for EE Specification in the Adult *Drosophila* Midgut

Wild-type, *sina*, or *phyl* homozygous mutant MARCM clones (GFP, green) examined on day 10 after clone induction (ACI).

(A–B') Clones co-stained with anti-Pros (red). (A and A') A wild-type *FRT2A* clone. (B and B') A *sina*² *FRT2A* clone. Note the absence of Pros⁺ cells in *sina* mutant clones (dashed lines and the separated red channels).

(C) The proportion of Pros⁺ cells per clone in wild-type and *sina* mutant clones on days 7–10 ACI. Mean ± SEM. n = 10 for *FRT 2A* clones, n = 24 for *sina*² clones, n = 16 for *FRT 80B* clones, and n = 22 for *sina*³ clones. ****p < 0.0001 (Student's t test).

(D and D') A *sina*² clone co-stained with anti-Pdm1 (dashed lines and the separated red channels).

(E and E') *phyl*²³⁶⁶ *FRT42D* mutant clones co-stained with anti-Dl (white). The yellow arrowhead indicates a *phyl* mutant cell positive for Dl expression.

(F) *phyl*²³⁶⁶ *FRT42D* mutant clones co-stained with anti-Pros (red). There were no Pros⁺ cells within the mutant clones.

(G–I) Knockdown of *phyl* in *esg*⁺ cells causes the loss of Pros⁺ cells (red) in the midgut. (G) control midgut. (H and I) *phyl*-RNAi midgut. Crosses were made at room temperature and midguts were dissected 10 days after eclosion.

(J) The percentages of Pros⁺ cells in *esg*>*GFP* and *esg*>*phyl*-RNAi midguts. Mean ± SEM. n = 14 for wild-type control midgut, n = 12 for *phyl*-RNAi#1 midgut, n = 15 for *phyl*-RNAi#2 midgut. ****p < 0.0001 (Student's t test).

Scale bars, 20 μm. See also Figures S1 and S2.

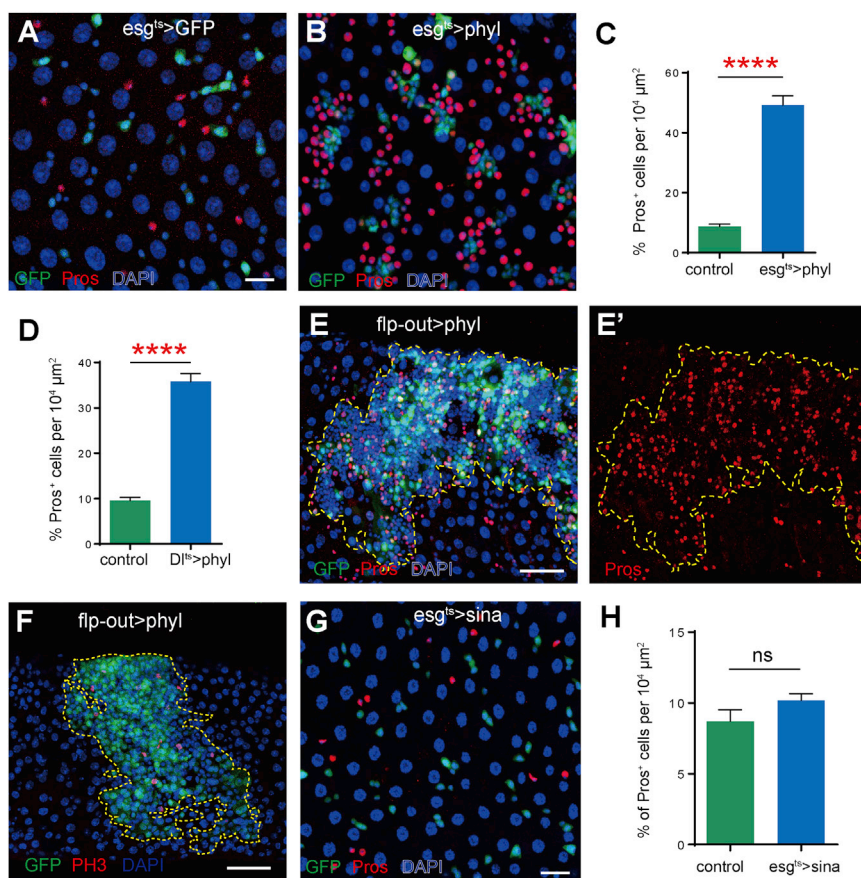


Figure 2. Phyl, but Not Sina, Acts as a Limiting Factor for EE Cell Fate Specification

(A and B) Conditional overexpression of *phyl* in *esg*^{ts} cells for 7 days resulted in excessive EEs (anti-Pros, red) in the midgut.

(C) The percentages of Pros⁺ cells in the epithelia of *esg*^{ts}>GFP and *esg*^{ts}>*phyl* midguts. Mean ± SEM. n = 15 for *esg*^{ts}>GFP midguts, and n = 16 for *esg*^{ts}>*phyl* midguts. ****p < 0.0001 (Student's t test).

(D) Conditional overexpression of *phyl* in Dl^{ts} cells for 7 days also produced excessive EEs. The percentage of Pros⁺ cells in midguts of indicated genotypes. Mean ± SEM. n = 23 for *Dl*^{ts}>GFP midguts, and n = 22 for *Dl*^{ts}>*phyl* midguts. ****p < 0.0001 (Student's t test).

(E and E') A flp-out clone (marked by GFP, green) with *phyl* overexpression co-stained with anti-Pros (red). Dashed lines depict the clone margin.

(F) The *phyl* overexpression flp-out clones (green) co-stained with anti-PH3 (red).

(G) Epithelium of *esg*-GAL4^{ts}>*sina* midgut stained with anti-Pros (red).

(H) Quantitative data on the percentages of Pros⁺ cells in the epithelia *esg*^{ts}>GFP and *esg*^{ts}>*sina* midguts. n = 15 for wild-type control midguts, n = 23 for *u-sina* midguts. Scale bars: (A [also applies to B] and G) 20 μm; (E and F) 50 μm. See also Figure S3.

epithelium. But unlike *sina*, *phyl* has additional roles in promoting ISC proliferation. It is noteworthy that although only posterior midgut regions were shown for the functional studies of *sina* and *phyl*, both genes are essential for EE generation along the length of the midgut, including anterior, middle, and posterior midgut regions.

Phyl, but Not Sina, Acts as a Limiting Factor for EE Cell Fate Specification

To evaluate whether *phyl* is sufficient to induce EE fate specification, we overexpressed *phyl* using the temperature-inducible GAL4-UAS expression system (McGuire et al., 2004). We found that conditional overexpression of *phyl* for 7 days in adult both ISCs and EBs using the *esg*-GAL4^{ts} (*esg*-GAL4, *Tub*-GAL80^{ts}) driver was sufficient to induce excessive production of EEs (Figures 2A–2C). Further, the continuous accumulation of EEs in the midgut epithelium eventually led to the development of multilayered EE-like tumors by around 2 weeks (not shown). Conditional overexpression of *phyl* using an ISC-specific driver, *Dl*-GAL4^{ts}, also induces extra production of EEs, albeit to a less pronounced extent than in the *esg*-GAL4; UAS-*phyl* flies (Figure 2D). Interestingly, conditional overexpression of *phyl* in Notch-activated EBs using *Su(H)Gbe*-GAL4^{ts}

blocked EB differentiation, induced re-entry into mitosis, and caused some of these accumulated EBs to differentiate into EEs (Figure S4), although normally the Notch-activated EBs are post-mitotic and only differentiate into ECs. This suggests that Phyl expression is able to force EC-committed EBs to re-enter the cell cycle and to promote differentiation into EE fate instead. To determine whether this EE-specification-promoting effect occurs in a lineage-autonomous or a non-lineage-autonomous manner, we overexpressed *phyl* in a clonal fashion using a flp-out cassette technique (Struhl and Basler, 1993). We generated clones comprised exclusively of *phyl*-overexpressing cells (marked by GFP). Strikingly, there was a massive accumulation of Pros⁺ EE cells and Dl^{ts} ISC-like cells within these clones, but the population and distribution of EE cells outside the clones remained normal (Figures 2E and S5). It is thus clear that the overexpression of *phyl* was sufficient to induce lineage-autonomous specification of EE cell fate. Consistent with our finding that *phyl* is required for ISC proliferation (Figures 1E and 1F), the overexpression of *phyl* also significantly increased ISC proliferation in a lineage-autonomous manner, as revealed by the significantly increased proportion of mitotic cells in these clones (Figure 2F). The ISC cell proliferation and EE cell specification

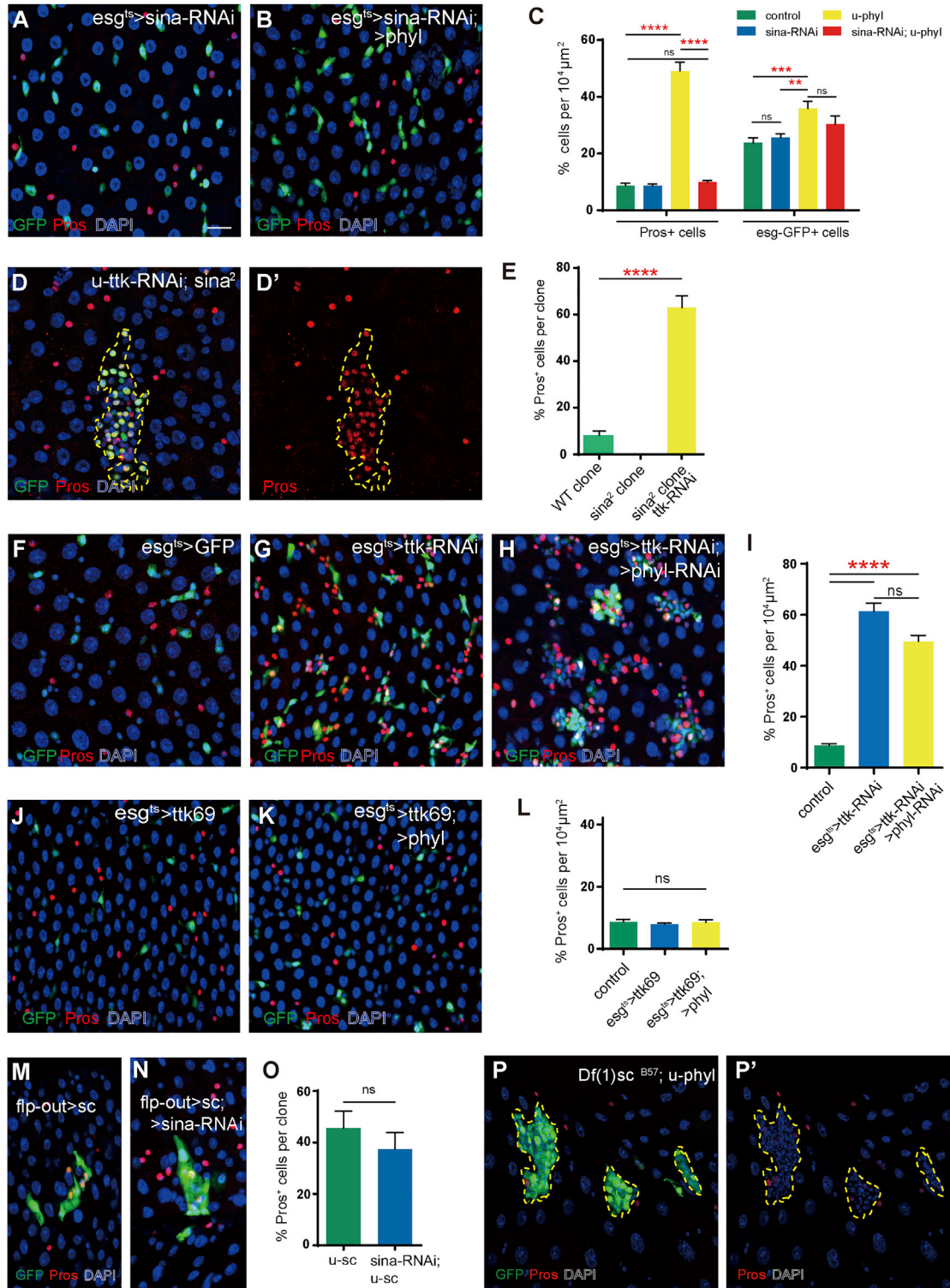


Figure 3. Epistatic Relationships among Sina, Phyl, Ttk69 and AS-C complex in Regulating EE Specification

(A and B) Midgut epithelia of indicated genotypes stained with anti-Pros (red). Flies were shifted to the restrictive temperature for 7 days before analysis. GFP, green.

(legend continued on next page)



effects of *phyl* together caused the rapid development of EE-like tumors in all the *phyl* overexpression clones (Figures 2E and 2F).

Using a similar approach, we also conditionally overexpressed *sina* in ISCs and EBs. *sina* overexpression did not cause any obvious abnormalities in either the ISC or EE population (Figures 2G and 2H), suggesting that *sina* only plays a permissive role for EE specification, and *phyl* is not only permissive but also instructive for EE specification from ISCs. Therefore, *phyl* seems to act as a limiting factor for EE fate specification from ISCs.

Similar to the phenotypes resulting from *phyl* overexpression, the loss of *ttk69* also causes excessive ISC proliferation and unidirectional generation of EEs and is also able to induce EC-committed EBs to re-enter mitosis and induce their differentiation into EE fate instead. Conversely, similar to *phyl* ablation, the overexpression of *ttk69* causes ISC quiescence and failure of EE differentiation (Wang et al., 2015). These phenotypic similarities support the idea that *phyl* and *ttk69* function in a common regulatory pathway to control EE specification.

Epistatic Relationships among Sina, Phyl, Ttk69 and AS-C complex in EE Specification

The similar requirement of Sina, Phyl, and Ttk69 for EE specification strongly suggests that the Sina-Phyl-Ttk69 protein complex, which is involved in eye and SOP development, may also be involved in the regulation of EE specification in the *Drosophila* midgut. If indeed Sina functions as an ubiquitin ligase and Phyl functions as an adaptor for recruitment, ubiquitination, and degradation

of Ttk69, the excessive EE phenotype caused by *phyl* overexpression should be dependent on *sina* activity. Recall that we earlier showed that the conditional overexpression of *phyl* in adult *esg*⁺ cells for 7 days effectively induced the generation of excessive EEs in the epithelium (Figure 2B). However, this phenotype was completely suppressed when *sina* was depleted via RNAi (Figures 3A–3C). Therefore, the ability of *phyl* to induce EE specification is dependent on *sina* activity. As an extra note, we found that the slight increase in of *esg*>GFP⁺ cells following *phyl* overexpression was not effectively suppressed by *sina*-RNAi (Figures 3A–3C), indicating that the function of *phyl* in promoting ISC proliferation is likely independent of *sina*.

We next tested the epistatic relationships between *ttk69* and *sina/phyl*. If Sina/Phyl functions to degrade Ttk69, Ttk69 should be downstream of Sina/Phyl in regulating EE specification (therefore genetically epistatic to *sina/phyl*). Recall that *sina*² mutant clones failed to generate any EEs (Figure 1B). However, the co-depletion of *ttk* in *sina*² mutant clones caused EE tumor formation in a lineage-autonomous manner (Figures 3D and 3E), a phenotype virtually identical to that resulting from *ttk* depletion alone (Wang et al., 2015). Therefore, *ttk69* is epistatic to *sina* in regulating EE specification. Similarly, we found that *ttk* is also epistatic to *phyl*. Depleting *phyl* via RNAi could not suppress the excessive EE phenotype caused by conditional depletion of *ttk* in *esg*⁺ cells (Figures 3F–3I), but overexpression of *ttk69* was sufficient to prevent excessive EE phenotype caused by conditional overexpression of *phyl* (Figures 3J–3L). These results demonstrate that *ttk69* is genetically downstream of *sina/phyl* in EE specification. The epistatic

(C) The percentages of Pros⁺ and GFP⁺ cells in the epithelia of indicated genotypes. Mean ± SEM. n = 15 for *esg*^{ts}>GFP control, n = 14 for *esg*^{ts}>*sina*-RNAi, n = 16 for *esg*^{ts}>*phyl*, and n = 12 for *esg*^{ts}>*sina*-RNAi; *u-phyl* midguts. **p < 0.01, ***p < 0.001, ****p < 0.0001 (Student's t test). ns, no significant difference.

(D and D') ISC clones of indicated genotypes co-stained with anti-Pros (red). Note the accumulation of Pros⁺ cells in *sina*² *ttk*-RNAi clones (dashed lines and the separated red channels).

(E) Quantitative data on the percentages of Pros⁺ cells in the clones shown in (D and D'). Mean ± SEM. n = 10 for wild-type *FRT2A* clones, n = 24 for *sina*² mutant clones, n = 12 for *ttk*-RNAi; *sina*² mutant clones. ****p < 0.0001 (Student's t test).

(F–H) Midgut epithelia of (F) *esg*^{ts}>GFP, (G) *esg*^{ts}>*ttk*-RNAi, and (H) *esg*^{ts}>*ttk*-RNAi; *phyl*-RNAi stained with anti-Pros (red). Flies were shifted to restrictive temperature for 7 days before analysis.

(I) Quantitative data on the percentages of Pros⁺ cells in the epithelia shown in (G–H). Mean ± SEM. n = 15 for *esg*^{ts}>GFP, n = 16 for *esg*^{ts}>*ttk*-RNAi, and n = 10 for *esg*^{ts}>*ttk*-RNAi; *phyl*-RNAi midguts. ****p < 0.0001 (Student's t test).

(J and K) Midgut epithelia of (J) *esg*^{ts}>UAS-*ttk69* and (K) *esg*^{ts}>UAS-*ttk69*; UAS-*phyl* stained with anti-Pros (red). Flies were shifted to restrictive temperature for 7 days before analysis.

(L) Quantitative data on the percentages of Pros⁺ cells in the epithelia shown in (K and L). Mean ± SEM. n = 15 for *esg*^{ts}>GFP controls, n = 19 for *esg*^{ts}>UAS-*ttk69*, and n = 15 for *esg*^{ts}>UAS-*ttk69*; UAS-*phyl* midguts. ns, no significant difference.

(M) Overexpression of *sc* by using the flp-out system (green), and the clone was stained with anti-Pros (red).

(N) Overexpression of *sc* in *sina*-RNAi flp-out clones (green) were stained with anti-Pros (red).

(O) The proportion of Pros⁺ cells per clone in clones of indicated genotypes on day 7 ACI. Mean ± SEM. n = 7 for *sc* overexpression clones, and n=7 for *sc* overexpression, *sina*-RNAi clones. ns, no significant difference.

(P and P') Overexpression of *phyl* in Df(1)*sc*^{B57} mutant clones failed to induce excessive EE cells (anti-Pros, in red). Dashed lines depict the clone margin.

Scale bar: 20 μm.



relationships among *sina*, *phyl*, and *ttk69* indicate that, similar to what occurs during *Drosophila* eye and SOP development, Sina/Phyl likely function to promote EE generation through the proteolytic degradation of Ttk69.

We next tested the epistatic relationships between AS-C genes and *sina/phyl*. Although *sina* mutant clones are devoid of EEs, we found that overexpression of *sc* in *sina*-RNAi clones was still able to induce EE specification within the clones (Figures 3M–3O), supporting the notion that *sc* is epistatic to *sina*. *Df(1)sc^{B57}* is a small chromosomal deficiency allele in which the entire AS-C genes are removed (Heitzler et al., 1996). Overexpression of *phyl* in induced *Df(1)sc^{B57}* clones failed to induce the supernumerary EE phenotype (Figure 3P). These clones are composed of small progenitor cells that do not have Pros expression (Figure 3P'). The occasional Pros⁺ cells found in the clones are likely due to residual activity of gene products. Collectively, these data demonstrate that AS-C genes are genetically downstream of *sina/phyl* and *ttk69*, and *ttk69* is genetically downstream of *sina/phyl* in EE specification. Therefore, a Sina-Phyl-Ttk69-AS-C regulatory axis controls EE specification in the *Drosophila* midgut.

Sina and Phyl Regulate Ttk69 Protein Stability

To test whether Sina/Phyl are able to regulate Ttk69 protein levels in the midgut, we used a highly specific antibody against Ttk69 (Wang et al., 2015) to monitor Ttk69 protein levels in the midgut following the manipulation of *sina/phyl* function. In wild-type midgut, Ttk69 was generally expressed in all epithelial cells, with the highest levels in ECs and the lowest levels in ISCs and EEs (Figure 4A) (Wang et al., 2015). *Myo1A-Gal4^{ts}* (*Myo1A-Gal4;Tub-GAL80^{ts}*), an EC-specific driver was used to conditionally ectopically express *phyl* in ECs. The impact of *phyl* expression on Ttk69 protein levels was analyzed 12, 24, and 48 hr after including *phyl* expression (Figures 4B–4D). Interestingly, downregulation of Ttk69 protein levels in ECs was observed as early as 12 hr (Figure 4B). Hardly any Ttk69 protein could be detected in ECs by 48 hr (Figures 4C and 4D). Therefore, the ectopic expression of *phyl* in ECs is able to rapidly downregulate Ttk69 protein levels in ECs. We also expressed a 3xFlag-tagged *ttk69* transgene in flip-out clones and examined the effect of *phyl* expression on Ttk69-Flag protein levels. Because *ttk69* overexpression inhibits ISC proliferation, Ttk69-Flag-overexpression clones hardly grew at all; many remained as single or double cell clones, and staining with anti-Flag antibody showed strong Ttk69-Flag protein expression in all of these clones (Figures 4E–4H). The addition of Phyl overexpression in Ttk69-Flag-overexpression clones caused clones to grow slightly bigger (Figures 4E–4H), indicating that the proliferation-inhibitory effect of Ttk69 is partially

suppressed by Phyl overexpression. Importantly, the Ttk69-Flag protein level was significantly downregulated in the Phyl/Ttk69-Flag co-overexpression clones, and no Ttk69-Flag protein could be detected in the majority of the cells of these clones (Figures 4F and 4G). Collectively, these results demonstrate that Phyl overexpression is sufficient to downregulate the Ttk69 protein level in a lineage-autonomous manner. This conclusion is consistent with the idea that Sina and Phyl function together to promote EE specification by inhibiting Ttk69 through proteolytic degradation.

Phyl Is Transiently Upregulated in EE Progenitor Cells and Is Positively Regulated by Sc

Given that *phyl* appears to be a limiting factor in EE specification, characterizing how *phyl* is regulated should deepen our understanding of the EE specification process. We therefore examined *phyl* expression using *phyl^{3.4}-GFP*, an *in vivo* GFP reporter driven by a 3.4 kb *phyl* promoter fragment (Pi et al., 2004). Interestingly, the expression of *phyl^{3.4}-GFP* was barely detectable in the midgut epithelium (Figure 5A). We also generated a polyclonal antibody against Phyl, and the anti-Phyl signal was also largely undetectable in the intestinal epithelium along the length of midgut, except that it was detected in the cytoplasm of some diploid cells in the copper cell (R3) region where gastric stem cells reside (Buchon et al., 2013; Strand and Micchelli, 2011; Wang et al., 2014). These Phyl⁺ diploid cells were co-stained with low levels of Pros and *esg>GFP*, indicating that they could be differentiating EE progenitor cells (Figures 5E and 5F). Regional differences in Phyl expression levels could be due to differential DI-Notch signaling activities, as Notch activity is known to be relatively low in the R3 region (Marianes and Spradling, 2013; Strand and Micchelli, 2011; Wang et al., 2014), and Phyl expression is negatively regulated by Notch (described later).

Despite failure to detect Phyl expression using both the GFP marker and the antibody in the anterior and posterior midgut, the functional requirement of *phyl* for EE specification along the length of the midgut suggests that *phyl* should be expressed there, but its expression level could be too low to be detected/reflected by antibody staining or by the transcriptional reporter. To test this hypothesis, we used a highly sensitive Tyramide Signal Amplification (TSA) method to amplify the reporter GFP signal and studied the *phyl^{3.4}-GFP* expression pattern. This analysis revealed that the majority of diploid cells, including ISCs and EEs, at both the anterior and posterior regions of the midgut, had active *phyl* transcription (Figure S6). It thus seems clear that Phyl is generally expressed in ISCs at low levels in both anterior and posterior midgut regions. This baseline Phyl activity is likely important for ISC



Myo1A^{ts}>GFP; u-*phyl*

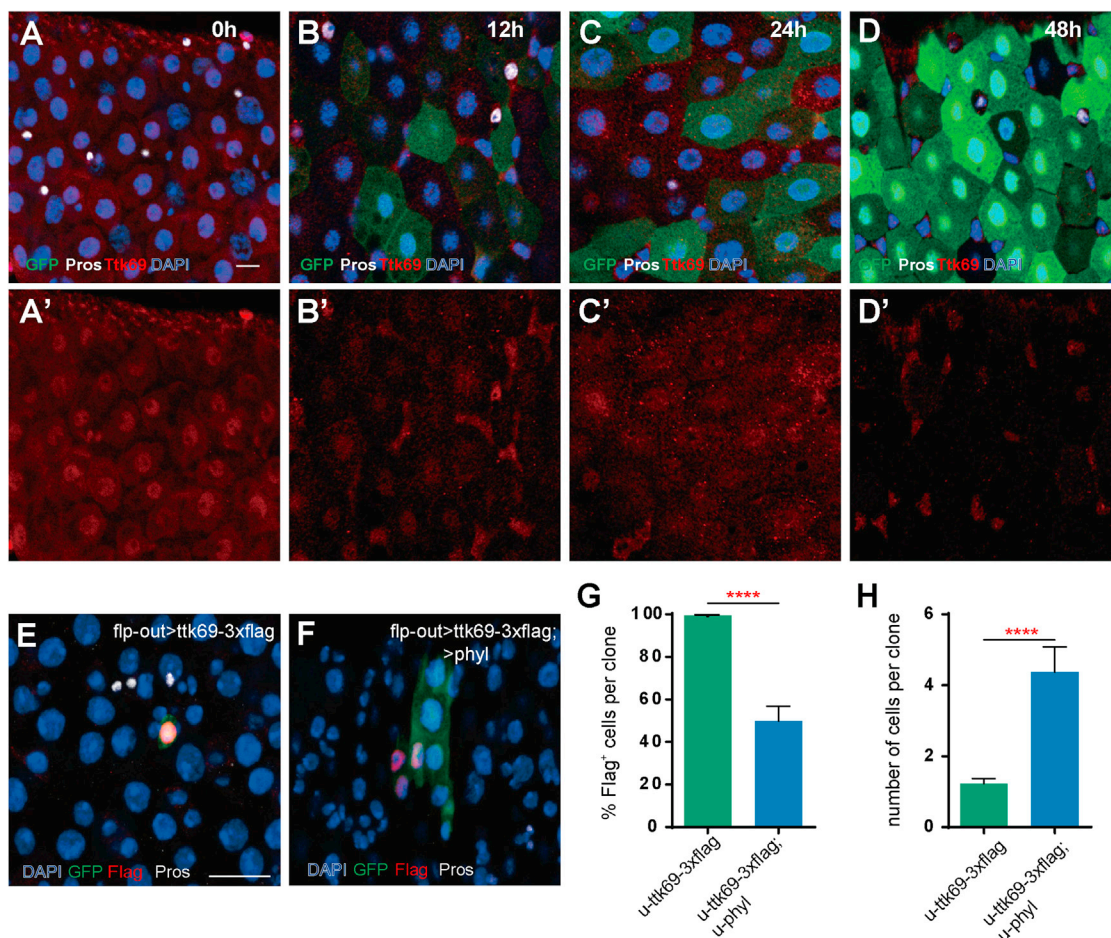


Figure 4. Sina and Phyl Regulate Ttk69 Protein Stability

(A–D) *phyl* was conditionally expressed in EC cells driven by *Myo1A*^{ts} and stained with anti-Ttk69 (red). (A and A') The midgut from *Myo1A-GAL4*^{ts}; *u-GFP* control flies. (B–D') The midguts from *Myo1A-GAL4*^{ts}; *u-GFP*; *u-phyl* flies treated at restrictive temperature for indicated length of time. Note that the Ttk69 protein level in small cells remained unaltered in all images, and the seemingly increased level in shown in (B–D) is because of increased signal contrast.

(E and F) flip-out GFP clones (green) with *u-ttk69-3xflag* overexpression (E) or with *u-ttk69-3xflag* and *u-phyl* co-overexpression (F) stained with anti-Flag antibody (red). Anti-Pros, white.

(G and H) The proportion of Flag⁺ cells (G) and the number of total cells per clone (H) in clones of indicated genotypes on 7 day ACI. Mean ± SEM. n = 35 for *ttk69-3xflag* overexpression clones, and n=22 for *ttk69-3xflag* and *phyl* both overexpression clones. ****p < 0.0001 (Student's t test).

Scale bars: (A) 10 μm (also applies to B–D); (E) 20 μm (also applies to F).

proliferation, as it was shown earlier that the proliferative ability of ISCs was strongly affected following the ablation of *phyl*.

We next examined whether *phyl* could be a transcriptional target of *sc* in the midgut, as *phyl* is known as a transcriptional target of *Sc* in external sensory organs (Pi et al., 2004). This is potentially interesting because *sc* is an essential AS-C gene known to be required for EE specifi-

cation that functions downstream of *ttk69* (Amcheslavsky et al., 2014; Bardin et al., 2010; Wang et al., 2015). As shown above, *phyl* expression was barely detectable in normal intestinal epithelium by either anti-Phyl staining or the *phyl*^{3,4}-GFP reporter. However, the conditional overexpression of *sc* in ISCs for 48 hr using *Dl-Gal4* rapidly induced *phyl* expression in progenitor cells, revealed by either anti-Phyl staining or the GFP reporter (Figure 5B

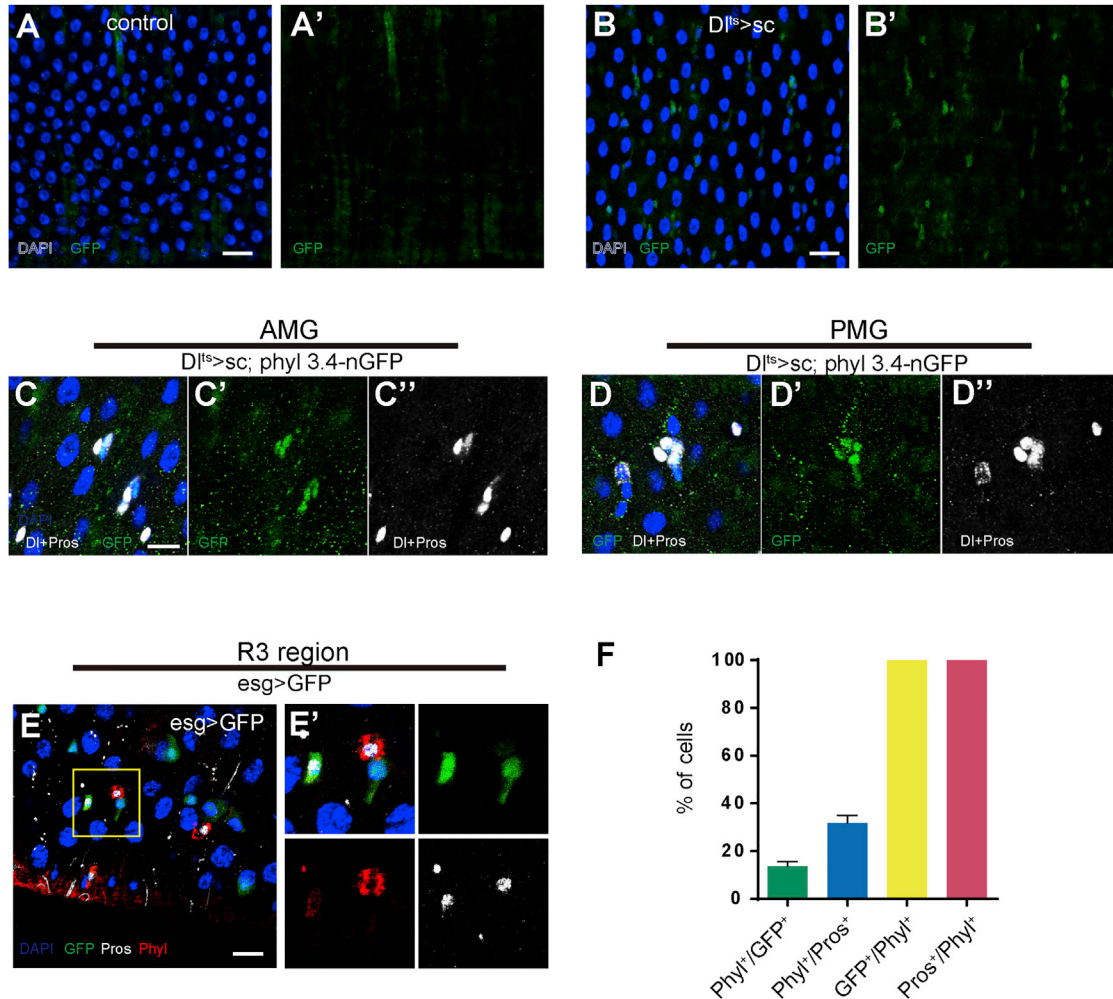


Figure 5. Phyl Is Transiently Upregulated in EE Progenitor Cells and Is Positively Regulated by Sc

(A–D') Midguts of indicated genotypes stained with anti-GFP (green). (A) Flies of *phyl3.4-nGFP*. (B) Flies of *DL-GAL4^{ts};u-sc, phyl3.4-nGFP*. Flies were shifted to restrictive temperature for 48 hr before analysis. Note that non-specific staining occurred on muscle fibers. Midguts of *DL-GAL4^{ts};u-sc, phyl3.4-nGFP* stained with DL and Pros antibody (white) in both the anterior (C) and the posterior (D) midgut regions.

(E) Flies of *esg>GFP* stained with anti-Pros (white) and anti-Phyl (red) in R3 region. Note that a high expression level of Phyl protein was observed in low-level GFP and Pros⁺ cells.

(F) Quantification of the percentage of indicated cells in R3 region of the midguts of *esg>GFP* flies. n = 4–6 midguts.

Scale bars: (A, B, and E) 20 μm; (C and D) 10 μm. See also Figure S4.

compared with 5A, and data not shown). Co-staining with Pros and DL markers revealed that, in both anterior and posterior midgut, the highest Phyl expression occurred in DL^{low} and Pros^{low} cells, which are likely differentiating EEs, and its expression became diminished in Pros^{high} cells (Figures 5C and 5D). These observations suggest that Sc is able to transcriptionally activate *phyl* in the midgut progenitor cells. Taking this into consideration, the initial activation of Phyl could reinforce its expression via a positive feedback mechanism mediated by Sina-Phyl-Ttk69 and Sc, which may ensure rapid accumulation of the

EE-determination factor Pros for EE specification and maturation. This positive feedback regulation of Phyl during EE differentiation is also consistent with the notion that Phyl seems to be accumulated at its highest levels in differentiating EEs.

Phyl Is Negatively Regulated by Notch

The binary fate choice of ISCs is primarily regulated by DL-Notch signaling. As reported previously, loss of Notch in ISCs causes ISC-like and EE-like tumors (Figure 6A). Forced activation of Notch in ISCs, on the other hand,

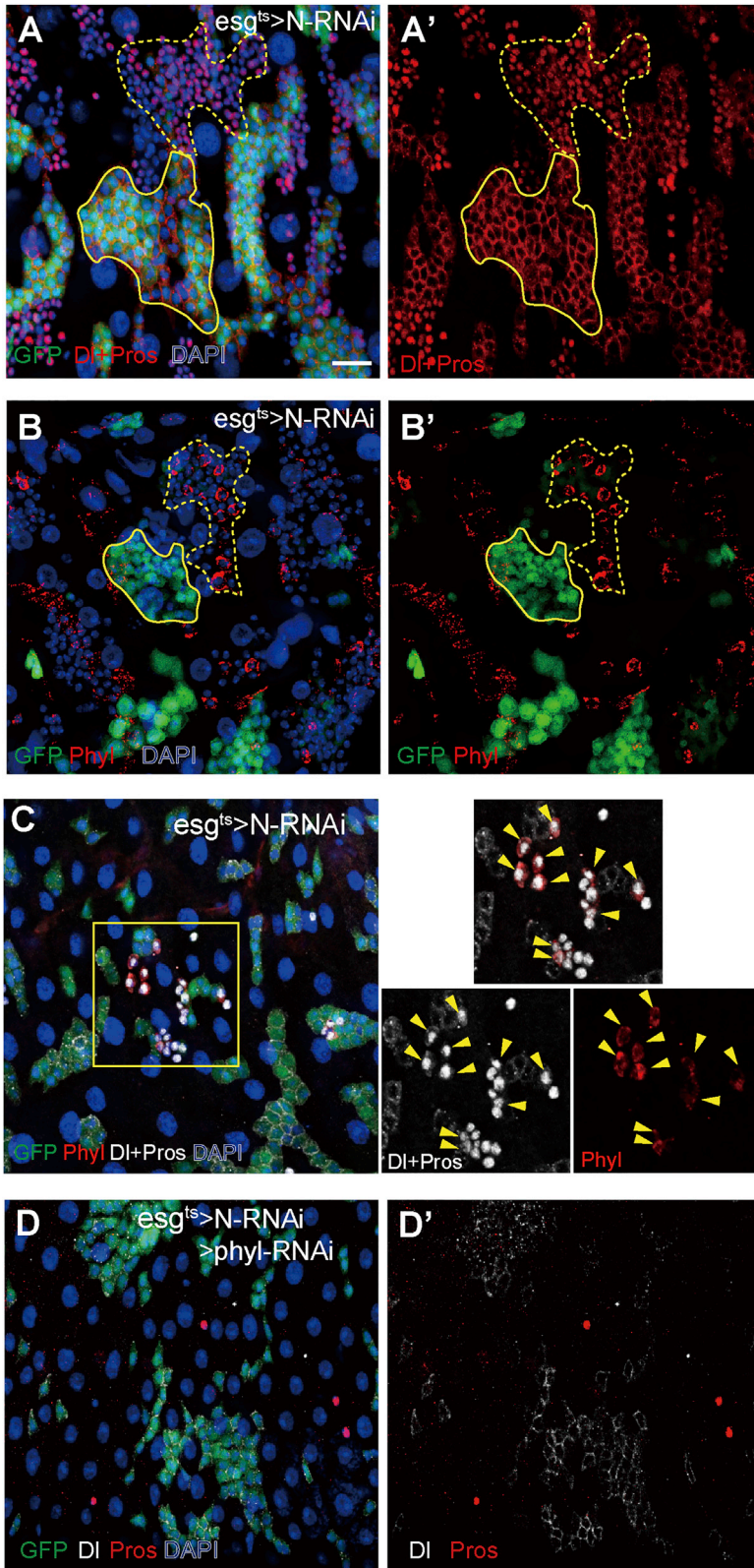


Figure 6. Phyl Is Negatively Regulated by Notch

(A and A') Midguts of *esg^{ts}>N-RNAi* stained with anti-Dl and anti-Pros in red. Flies were shifted to restrictive temperature for 14 days before analysis. Note that ISC-like tumors (high GFP, solid line) and EE-like tumors (low GFP, dashed line) were induced. (B and B') Flies of *esg^{ts}>N-RNAi* stained with anti-Phyl. Note that a high expression level of cytoplasmic Phyl protein (red) was observed in a portion of cells within the EE-like tumor (low GFP, dashed line) but not in the ISC-like cells (high GFP, solid line).

(C) Flies of *esg^{ts}>N-RNAi* stained with anti-Phyl (red) and Dl, Pros (white). Note the Phyl⁺ cells were mainly Pros⁺ and Dl^{+/low} cells (yellow arrowheads).

(D and D') Flies of *esg^{ts}>N-RNAi; phyl-RNAi* stained with anti-Dl (white) and anti-Pros (red). Note that EE-like tumors disappeared when *Notch* and *phyl* were co-depleted.

Scale bar: 20 μm.

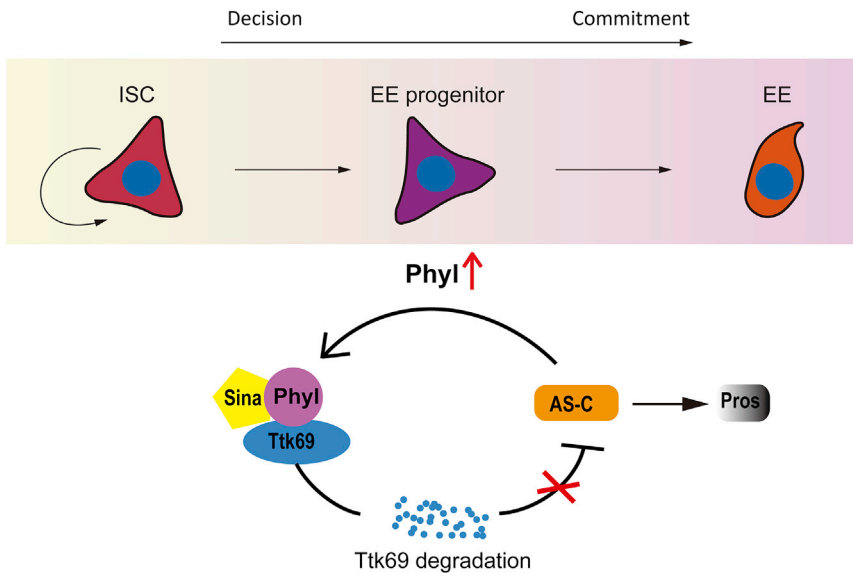


Figure 7. A Schematic Model for EE Specification Driven by the Positive Feedback Regulatory Circuit Composed of Sina/Phyl, Ttk69, and Sc

In EE progenitor cells derived from ISCs, Phyl is upregulated, which links EE-repressor Ttk69 to the E3 ubiquitin ligase Sina for degradation. Ttk69 degradation results in the derepression of AS-C genes, which subsequently induces the expression of EE-determination factor Pros to promote EE specification. The expression of Sc also induces Phyl expression, thereby forming a positive feedback regulatory circuit that continuously drives Phyl expression, Ttk69 degradation, and Pros accumulation, ultimately leading to EE commitment.

unidirectionally induces ISC differentiation into ECs (Micchelli and Perrimon, 2006; Ohlstein and Spradling, 2006, 2007), indicating that Notch is inactive or at low levels during EE generation. To test the potential regulatory relationships between Notch and Phyl, we examined Phyl expression in *esg>Notch-RNAi* epithelia. Although Phyl expression was hardly detectable in the anterior and posterior midgut, its expression was readily detectable in a subset of Pros⁺ tumor cells in *esg>Notch-RNAi* intestine (Figure 6B). Co-staining with DI and Pros markers revealed that Phyl⁺ cells were mainly Pros⁺ and DI^{+/low} cells (Figure 6C and arrowheads in insets). Because differentiation into EE is accompanied by downregulation of DI expression and initiation of Pros expression, these Pros⁺ and DI⁺ cells are likely early EEs that are still in the process of differentiation toward maturation. It thus further reinforces the notion that Phyl is transiently upregulated in differentiating EEs. This transient upregulation of Phyl may lead to activation of the positive feedback loop for rapid accumulation of Pros in these cells and consequently EE commitment. To functionally test whether *phyl* expression is required for EE-like tumor cell generation, we co-depleted *Notch* and *phyl* in ISCs and studied the consequences. As a result, co-depletion of *phyl* caused the failure of EE-like tumor formation, although ISC-like tumors could still be formed (Figure 6D). The size of these *phyl*-RNAi *N*-RNAi ISC-like tumors appeared smaller than *N*-RNAi ISC-like tumors, but the difference was not statistically significant (Figure S7). It is thus possible that the cell proliferation activity of *phyl* could be dependent on Notch. We conclude that Phyl is normally suppressed by Notch, and loss of Notch causes derepression of Phyl, which drives continuous EE generation, leading to EE-like tumor

formation. It is noteworthy that many *Notch* mutant cells, including all DI⁺ ISC-like cells, do not show any detectable Phyl expression, suggesting that additional mechanisms are involved to regulate Phyl expression at the early stages of fate decision in ISCs.

DISCUSSION

Our results collectively suggest a regulatory circuit in differentiating progenitors that drive EE fate commitment. Normally Phyl is suppressed by Notch. In EE progenitor cells that are Notch^{low} or inactive, Phyl is transiently upregulated, which acts as an adaptor protein to bring Ttk69 to the E3 ubiquitin ligase Sina for proteolytic degradation. The expression of the Ttk69 target gene *sc* is subsequently derepressed, which then induces expression of the EE fate determination factor Pros. Notably, expression of *sc* also induces *phyl* expression, thereby forming a positive feedback circuit that drives Ttk69 degradation and Pros accumulation, ultimately specifying EE fate (Figure 7).

Regulatory circuits with feedback mechanisms are frequently used by multi-celled organisms to control the proportional generation of differentiated cell subtypes and for the homeostatic control of tissue maintenance and regeneration (Hsu and Fuchs, 2012; Tata and Rajagopal, 2016). In the *Drosophila* midgut, epithelial damage induces feedback regulation between ISCs and their progeny that promotes activation of ISCs for epithelial repair (Chen et al., 2016; Jiang et al., 2009). It has also been shown that differentiated EEs send feedback signals such as Slit molecules to ISCs to prevent excessive EE generation



(Biteau and Jasper, 2014), but a recent study does not support the existence of such a feedback mechanism (Salle et al., 2017). Here, we identify a positive feedback circuit that functions in the process of EE specification. The engagement of this type of positive feedback circuit could conceivably serve several purposes. First, such a circuit could allow the rapid accumulation of fate regulators like Pros to a critical threshold for cell fate commitment, perhaps functioning to overcome the influence of proteolytic degradation of the fate regulators. Second, once induced, fate regulators may need to be present continuously to specify cell fate, and a positive feedback mechanism could ensure such an ongoing expression. Third, activation of this type of positive feedback circuit may also effectively prevent unwanted cell fate reversion. It is known that many committed progenitor cells are still able to change (revert) their fate under certain circumstances, as with the enteroendocrine progenitor cells in the mouse small intestine that can act as a reservoir for ISCs in response to ISC loss. The enterocyte-committed EBs in the fly ISC lineage also have the potential to revert their EE fate specification, such as following *ttk69* depletion (Wang et al., 2015), or *phyl* overexpression reported in this study. In this context, the engagement of a positive feedback circuit at the start of EE specification could be an effective strategy to continuously ensure faithful commitment to the EE fate, especially under normal conditions.

How is the binary fate decision of ISCs, which directs the proportional generation of EC and EE from ISCs, regulated? A recent study from our group demonstrates that a transient activation of Sc in ISCs directs the generation of EEs from self-renewing ISCs (Chen et al., 2017). Although the current study primarily focuses on the role of Phyl in a positive feedback loop in differentiating EEs, Phyl could have an earlier function in ISCs to regulate Sc expression, and consequently cell proliferation and cell fate decisions. In addition, Phyl overexpression is able to induce many ISC-like cells, similar to that caused by the loss of Notch. A negative role for *phyl* in Notch signaling has been observed in developing eye imaginal discs, in which *phyl* is required for endocytic degradation of activated Notch (Nagaraj and Banerjee, 2009). Considering that Notch negatively regulates both *sc* and *phyl* transcription in the midgut, it is possible that the antagonistic activities of Phyl and Notch could participate in regulation of Sc and consequently cell fate decisions in ISCs.

Post-transcriptional regulation of Ttk by Sina and Phyl is known to determine neural cell fate versus non-neural cell fate in eye and sensory organ development, highlighting that Ttk-based mechanisms are used frequently in multiple developmental processes to regulate alternative cell fate decisions in *Drosophila*. Sina is an evolutionarily conserved

E3 ubiquitin ligase. Similarly, BTB domain-containing proteins like Ttk are present in all eukaryotes (Perez-Torrado et al., 2006). Although mammals appear to have no Phyl homologs, this does not exclude the possibility that they may have functional counterpart(s). The loss of a mammalian *sina* gene, *siah2*, suppresses the neuroendocrine tumor phenotype in a mouse model of prostate cancer (Qi et al., 2010). It is therefore possible that protein complexes similar to Sina-Phyl-Ttk69 maybe function in diverse mammalian tissues, including for example in the epithelium inner lining of the digestive tract, to regulate cell fate decisions.

In short, this study identified a regulatory circuit composed of Sina-Phyl-Ttk69 and Sc that drives EE commitment from ISCs. The earliest event that initiates EE differentiation from ISCs, that is, the event that causes Notch inactivation and initial Phyl expression, is still unclear, but it is possibly linked to Numb-mediated symmetric cell division and other environmental cues (Salle et al., 2017). We propose that the engagement of a positive feedback circuit to drive cell fate specification, as revealed in the present study, may be a common mechanism employed to ensure faithful cell fate determination from progenitor cells in diverse organisms, including mammals.

EXPERIMENTAL PROCEDURES

Fly Strains

The following fly stocks were used in this study: *sina*² *FRT2A* (BDSC, #30724); *sina*³ *FRT80B* (BDSC, #26270); *FRT42D phyl*²³⁶⁶ (BDSC, #30723); *phyl*²²⁴⁵ (Kyoto Stock Center, #108363); *FRT2A, FRT80B, FRT42D, Tub-Gal80^S, UAS-ttk69, Myo1A-Gal4, UAS-Notch-RNAi*, and *Act<stop>Gal4* (all obtained from BDSC); *esg-Gal4* and *UAS-GFP*, (gift from Shigeo Hayashi, RIKEN Center for Development Biology, Japan); *UAS-phyl-RNAi#1* (BDSC, #29433); *UAS-phyl-RNAi#2* (VDRC, v35469); *UAS-phyl* (BDSC, #52015); *UAS-sina.myc* (BDSC, #30931); *UAS-sina-RNAi* (VDRC, v100691); *UAS-sc* (BDSC, #26687); *phyl*³⁻⁴-*nGFP* (a gift from Haiwei Pi, Department of Life Science, Chang-Gung University, Taiwan; Pi et al., 2004); *Su(H)-Gal4* and *Dl-Gal4* (a gift from Xiankun Zeng and Steven Hou, National Cancer Institute, USA; Zeng et al., 2010); *UAS-N^{icd}* (a gift from Ting Xie, Stowers Institute for Medical Research, USA); *UAS-sc-3HA* (Fly ORE, F000085) (Bischof et al., 2013). *UAS-ttk69-3xflag* was generated in the course of the present study. Briefly, the cDNA of *ttk69* was cloned into the gateway attB-PUAST-3xflag vector (Drosophila Genomics Resource Center), and the plasmid was injected into embryos of attP40 flies.

Mosaic Analysis

GFP-marked clones in *Drosophila* midgut epithelium cells were generated using the MARCM system (Lee and Luo, 1999) and the flip-out technique (Struhl and Basler, 1993), as previously described (Lin et al., 2008, 2010; Xu et al., 2011). Female flies (between 3 and 5 days old) of a given genotype were exposed to heat-shock



treatment for 1 hr at 37°C in a water bath. After the heat-shock treatment, flies were cultured at 25°C with regular food and were analyzed 4–14 days later.

Temperature Shift Assay

Flies carrying *esg^{ts}* (*esg-Gal4*, *Tubulin-Gal80^{ts}*), *Dl^{ts}*, or *Su(H)^{ts}* were crossed with appropriately matched transgenic flies contain *UAS-transgenes* at 18°C (Wang et al., 2015). Female flies (between 3 and 5 days old) of a given genotype were shifted from 18°C to 29°C and cultured with regular food that was refreshed every 2 days. Dissection and analysis were performed 7 days after the initial temperature shift or at other time points, as specified in the text.

Generation of Phyl Antisera

Polyclonal antibody directly against Phyl was generated in rabbit by using the synthetic peptide: TPAPIVYSKRRASRRSASVSC. The cysteine residue at the C terminus of the peptide was able to conjugate keyhole limpet hemocyanin. Serum obtained from immunized rabbit was purified by antigen affinity chromatography. Purified antiserum was used at a final dilution of 1:300.

Immunostaining

Immunostaining of *Drosophila* midgut was performed as previously described (Lin et al., 2008). The following primary antibodies were used in this study: mouse anti-Dl (DSHB, C594.9B; 1:100); mouse anti-Pros (DSHB, MR1A; 1:100); rabbit anti-Tachykinin (a gift from Dick Nassel, Stockholm University, Sweden; 1:3,000); rabbit anti-Pdm1 (a gift from Xiaohang Yang, Zhejiang University, China; 1:1,000); mouse anti-phospho-Histone H3 (Cell Signaling Technology, #9706, 1:500); rabbit anti-GFP (Molecular Probes, A11122, 1:200); anti-Ttk69 (Wang et al., 2015); mouse anti-FLAG (Sigma, F1084; 1:300). Secondary antibodies were used in this study: goat anti-rabbit or anti-mouse IgGs conjugated to Alexa Fluor 488, 568, or Cy5 (Molecular Probes, A11034-A11036, A10524; 1:300). Signal amplification experiments were performed using a TSA kit (Invitrogen, TSA kit #22). Images were captured using a Nikon A1-R confocal microscope. All images were edited in Adobe Photoshop and were assembled in Adobe Illustrator.

SUPPLEMENTAL INFORMATION

Supplemental Information includes seven figures and can be found with this article online at <https://doi.org/10.1016/j.stemcr.2017.11.014>.

AUTHOR CONTRIBUTIONS

C.Y. and R.X. conceived and designed the experiments, analyzed the data, and wrote the manuscript. C.Y. performed the experiments.

ACKNOWLEDGMENTS

We thank the members of the fly community, as cited in Experimental Procedures, for generously providing fly strains and antibodies; the Bloomington *Drosophila* Stock Center (BDSC), the Kyoto Stock Center, the Vienna *Drosophila* RNAi Center (VDRC),

and Development Studies Hybridoma Bank (DSHB) for reagents; Xingting Guo for UAS-ttk69-Flag cloning, An-Ying Kang for micro-injections, John Snyder for editing the manuscript, and the lab members for comments and discussions. This work was supported by grants from the National Key Research and Development Program of China (2017YFA0103602) and the National Basic Research Program of China (2014CB850002) from the Chinese Ministry of Science and Technology.

Received: June 12, 2017

Revised: November 15, 2017

Accepted: November 16, 2017

Published: December 21, 2017

REFERENCES

- Amcheslavsky, A., Song, W., Li, Q., Nie, Y., Bragatto, I., Ferrandon, D., Perrimon, N., and Ip, Y.T. (2014). Enteroendocrine cells support intestinal stem-cell-mediated homeostasis in *Drosophila*. *Cell Rep.* 9, 32–39.
- Badenhorst, P. (2001). Tramtrack controls glial number and identity in the *Drosophila* embryonic CNS. *Development* 128, 4093–4101.
- Badenhorst, P., Finch, J.T., and Travers, A.A. (2002). Tramtrack cooperates to prevent inappropriate neural development in *Drosophila*. *Mech. Dev.* 117, 87–101.
- Bardin, A.J., Perdigoto, C.N., Southall, T.D., Brand, A.H., and Schweisguth, F. (2010). Transcriptional control of stem cell maintenance in the *Drosophila* intestine. *Development* 137, 705–714.
- Beebe, K., Lee, W.C., and Micchelli, C.A. (2010). JAK/STAT signaling coordinates stem cell proliferation and multilineage differentiation in the *Drosophila* intestinal stem cell lineage. *Dev. Biol.* 338, 28–37.
- Bischof, J., Bjorklund, M., Furger, E., Schertel, C., Taipale, J., and Basler, K. (2013). A versatile platform for creating a comprehensive UAS-ORFeome library in *Drosophila*. *Development* 140, 2434–2442.
- Biteau, B., Hochmuth, C.E., and Jasper, H. (2011). Maintaining tissue homeostasis: dynamic control of somatic stem cell activity. *Cell Stem Cell* 9, 402–411.
- Biteau, B., and Jasper, H. (2014). Slit/Robo signaling regulates cell fate decisions in the intestinal stem cell lineage of *Drosophila*. *Cell Rep.* 7, 1867–1875.
- Brand, A.H., and Perrimon, N. (1993). Targeted gene expression as a means of altering cell fates and generating dominant phenotypes. *Development* 118, 401–415.
- Buchon, N., Osman, D., David, F.P., Fang, H.Y., Boquete, J.P., Deplancke, B., and Lemaitre, B. (2013). Morphological and molecular characterization of adult midgut compartmentalization in *Drosophila*. *Cell Rep.* 3, 1725–1738.
- Carthew, R.W., and Rubin, G.M. (1990). Seven in absentia, a gene required for specification of R7 cell fate in the *Drosophila* eye. *Cell* 63, 561–577.
- Chen, J., Xu, N., Huang, H., Cai, T., and Xi, R. (2016). A feedback amplification loop between stem cells and their progeny promotes tissue regeneration and tumorigenesis. *Elife* 5, e14330.



- Chen, J., Xu, N., Wang, C., Huang, P., Huang, H., Jin, Z., Yu, Z., Cai, T., Jiao, R., and Xi, R. (2017). Transient Scute activation via a self-stimulatory loop directs enteroendocrine cell pair specification from self-renewing intestinal stem cells. *Nat. Cell Biol.* <https://doi.org/10.1038/s41556-017-0020-0>.
- Giesen, K., Hummel, T., Stollewerk, A., Harrison, S., Travers, A., and Klambt, C. (1997). Glial development in the *Drosophila* CNS requires concomitant activation of glial and repression of neuronal differentiation genes. *Development* **124**, 2307–2316.
- Graf, T., and Enver, T. (2009). Forcing cells to change lineages. *Nature* **462**, 587–594.
- Guo, M., Bier, E., Jan, L.Y., and Jan, Y.N. (1995). Tramtrack acts downstream of numb to specify distinct daughter cell fates during asymmetric cell divisions in the *Drosophila* PNS. *Neuron* **14**, 913–925.
- Heitzler, P., Bourouis, M., Ruel, L., Carteret, C., and Simpson, P. (1996). Genes of the Enhancer of split and achaete-scute complexes are required for a regulatory loop between Notch and Delta during lateral signalling in *Drosophila*. *Development* **122**, 161–171.
- Hsu, Y.C., and Fuchs, E. (2012). A family business: stem cell progeny join the niche to regulate homeostasis. *Nat. Rev. Mol. Cell Biol.* **13**, 103–114.
- Jiang, H., and Edgar, B.A. (2011). Intestinal stem cells in the adult *Drosophila* midgut. *Exp. Cell Res.* **317**, 2780–2788.
- Jiang, H., Patel, P.H., Kohlmaier, A., Grenley, M.O., McEwen, D.G., and Edgar, B.A. (2009). Cytokine/Jak/Stat signaling mediates regeneration and homeostasis in the *Drosophila* midgut. *Cell* **137**, 1343–1355.
- Kapuria, S., Karpac, J., Biteau, B., Hwangbo, D., and Jasper, H. (2012). Notch-mediated suppression of TSC2 expression regulates cell differentiation in the *Drosophila* intestinal stem cell lineage. *PLoS Genet.* **8**, e1003045.
- Lee, T., and Luo, L. (1999). Mosaic analysis with a repressible cell marker for studies of gene function in neuronal morphogenesis. *Neuron* **22**, 451–461.
- Li, S., Li, Y., Carthew, R.W., and Lai, Z.C. (1997). Photoreceptor cell differentiation requires regulated proteolysis of the transcriptional repressor Tramtrack. *Cell* **90**, 469–478.
- Li, S., Xu, C., and Carthew, R.W. (2002). Phyllopod acts as an adaptor protein to link the Sina ubiquitin ligase to the substrate protein tramtrack. *Mol. Cell Biol.* **22**, 6854–6865.
- Lin, G., Xu, N., and Xi, R. (2008). Paracrine Wingless signalling controls self-renewal of *Drosophila* intestinal stem cells. *Nature* **455**, 1119–1123.
- Lin, G., Xu, N., and Xi, R. (2010). Paracrine unpaired signaling through the JAK/STAT pathway controls self-renewal and lineage differentiation of *Drosophila* intestinal stem cells. *J. Mol. Cell Biol.* **2**, 37–49.
- Marianes, A., and Spradling, A.C. (2013). Physiological and stem cell compartmentalization within the *Drosophila* midgut. *Elife* **2**, e00886.
- McGuire, S.E., Mao, Z., and Davis, R.L. (2004). Spatiotemporal gene expression targeting with the TARGET and gene-switch systems in *Drosophila*. *Sci. STKE* **2004**, pl6.
- Micchelli, C.A., and Perrimon, N. (2006). Evidence that stem cells reside in the adult *Drosophila* midgut epithelium. *Nature* **439**, 475–479.
- Nagaraj, R., and Banerjee, U. (2009). Regulation of Notch and Wingless signalling by phyllopod, a transcriptional target of the EGFR pathway. *EMBO J.* **28**, 337–346.
- Ohlstein, B., and Spradling, A. (2006). The adult *Drosophila* posterior midgut is maintained by pluripotent stem cells. *Nature* **439**, 470–474.
- Ohlstein, B., and Spradling, A. (2007). Multipotent *Drosophila* intestinal stem cells specify daughter cell fates by differential notch signaling. *Science* **315**, 988–992.
- Okabe, M., Imai, T., Kurusu, M., Hiromi, Y., and Okano, H. (2001). Translational repression determines a neuronal potential in *Drosophila* asymmetric cell division. *Nature* **411**, 94–98.
- Ou, C.Y., Pi, H., and Chien, C.T. (2003). Control of protein degradation by E3 ubiquitin ligases in *Drosophila* eye development. *Trends Genet.* **19**, 382–389.
- Perdigoto, C.N., Schweisguth, F., and Bardin, A.J. (2011). Distinct levels of Notch activity for commitment and terminal differentiation of stem cells in the adult fly intestine. *Development* **138**, 4585–4595.
- Perez-Torrado, R., Yamada, D., and Defossez, P.A. (2006). Born to bind: the BTB protein-protein interaction domain. *Bioessays* **28**, 1194–1202.
- Pi, H., Huang, S.K., Tang, C.Y., Sun, Y.H., and Chien, C.T. (2004). Phyllopod is a target gene of proneural proteins in *Drosophila* external sensory organ development. *Proc. Natl. Acad. Sci. USA* **101**, 8378–8383.
- Pi, H., Wu, H.J., and Chien, C.T. (2001). A dual function of phyllopod in *Drosophila* external sensory organ development: cell fate specification of sensory organ precursor and its progeny. *Development* **128**, 2699–2710.
- Qi, J., Nakayama, K., Cardiff, R.D., Borowsky, A.D., Kaul, K., Williams, R., Krajewski, S., Mercola, D., Carpenter, P.M., Bowtell, D., et al. (2010). Siah2-dependent concerted activity of HIF and FoxA2 regulates formation of neuroendocrine phenotype and neuroendocrine prostate tumors. *Cancer Cell* **18**, 23–38.
- Quan, Z., Sun, P., Lin, G., and Xi, R. (2013). TSC1/2 regulates intestinal stem cell maintenance and lineage differentiation through Rheb-TORC1-S6K but independently of nutritional status or Notch regulation. *J. Cell Sci.* **126**, 3884–3892.
- Salle, J., Gervais, L., Boumard, B., Stefanutti, M., Siudeja, K., and Bardin, A.J. (2017). Intrinsic regulation of enteroendocrine fate by Numb. *EMBO J.* **36**, 1928–1945.
- Strand, M., and Micchelli, C.A. (2011). Quiescent gastric stem cells maintain the adult *Drosophila* stomach. *Proc. Natl. Acad. Sci. USA* **108**, 17696–17701.
- Struhl, G., and Basler, K. (1993). Organizing activity of wingless protein in *Drosophila*. *Cell* **72**, 527–540.
- Tang, A.H., Neufeld, T.P., Kwan, E., and Rubin, G.M. (1997). PHYL acts to down-regulate TTK88, a transcriptional repressor of neuronal cell fates, by a SINA-dependent mechanism. *Cell* **90**, 459–467.



Tata, P.R., and Rajagopal, J. (2016). Regulatory circuits and bi-directional signaling between stem cells and their progeny. *Cell Stem Cell* *19*, 686–689.

Wang, C., Guo, X., Dou, K., Chen, H., and Xi, R. (2015). Ttk69 acts as a master repressor of enteroendocrine cell specification in *Drosophila* intestinal stem cell lineages. *Development* *142*, 3321–3331.

Wang, C., Guo, X., and Xi, R. (2014). EGFR and Notch signaling respectively regulate proliferative activity and multiple cell lineage differentiation of *Drosophila* gastric stem cells. *Cell Res.* *24*, 610–627.

Xiong, W.C., and Montell, C. (1993). Tramtrack is a transcriptional repressor required for cell fate determination in the *Drosophila* eye. *Genes Dev.* *7*, 1085–1096.

Xu, N., Wang, S.Q., Tan, D., Gao, Y., Lin, G., and Xi, R. (2011). EGFR, Wingless and JAK/STAT signaling cooperatively maintain *Drosophila* intestinal stem cells. *Dev. Biol.* *354*, 31–43.

Zeng, X., Chauhan, C., and Hou, S.X. (2010). Characterization of midgut stem cell- and enteroblast-specific Gal4 lines in *Drosophila*. *Genesis* *48*, 607–611.

Zeng, X., and Hou, S.X. (2015). Enteroendocrine cells are generated from stem cells through a distinct progenitor in the adult *Drosophila* posterior midgut. *Development* *142*, 644–653.

Zernicka-Goetz, M., Morris, S.A., and Bruce, A.W. (2009). Making a firm decision: multifaceted regulation of cell fate in the early mouse embryo. *Nat. Rev. Genet.* *10*, 467–477.

Stem Cell Reports, Volume 10

Supplemental Information

**A Phyllopod-Mediated Feedback Loop Promotes Intestinal Stem Cell
Enteroendocrine Commitment in *Drosophila***

Chang Yin and Rongwen Xi

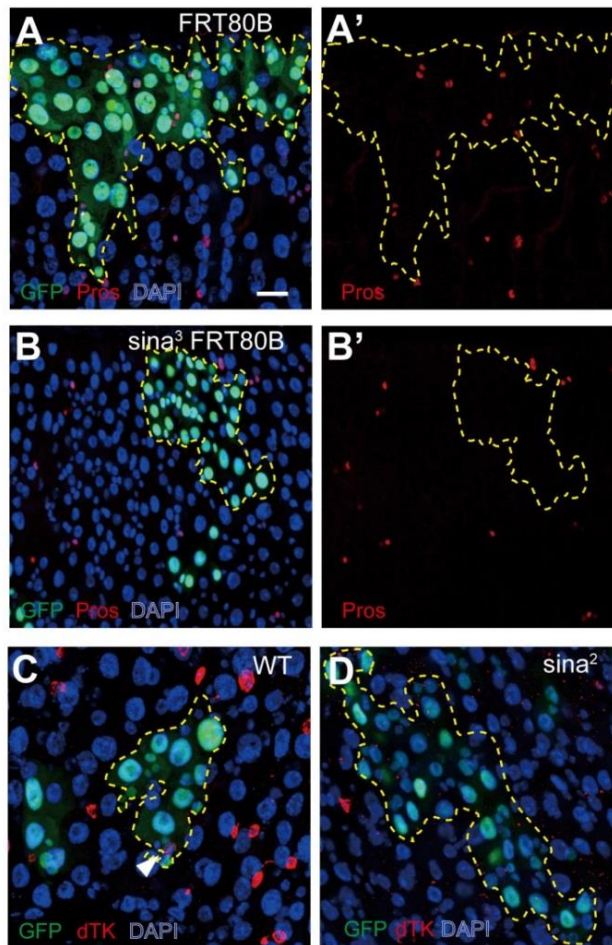


Fig. S1, Related to Figure 1. *sina* is required for EE cell fate specification.

Wild-type or *sina* homozygous mutant clones (GFP, green) were generated by the MARCM system and were examined on 10 day after clone induction (ACI).

(A-B') Clones co-stained with anti-Pros (red). (A,A') A wild-type *FRT80B* clone. (B,B') A *sina*³ *FRT80B* clone. Note the absence of Pros⁺ cells in *sina* mutant clones (dashed lines and the separated red channels).

(C-D) Clones co-stained with anti- dTK. (C) A wild-type clone. (D) A *sina*² clone. dTK⁺ cells were not observed in *sina* mutant clones.

Scale bar: 20 μm

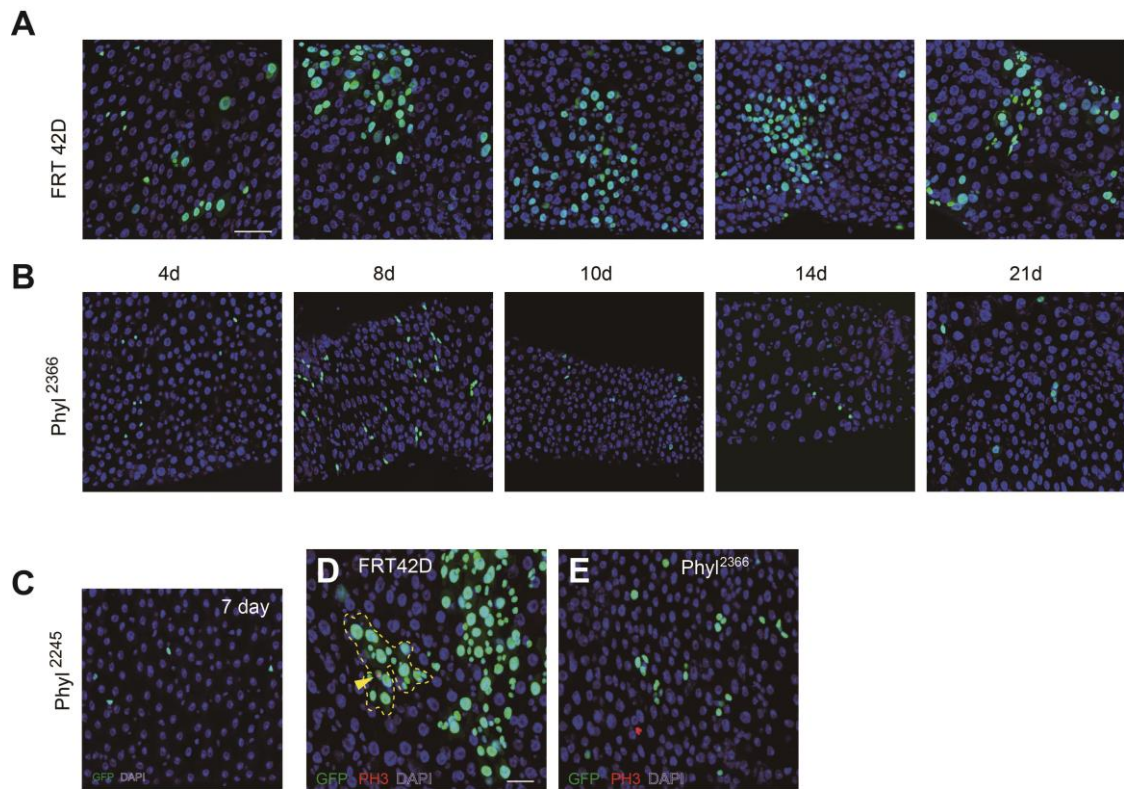


Fig. S2, Related to Figure 1. Clonal analysis of wild-type and *phyl* mutant cells in the midgut epithelia.

(A-B) GFP marked wild-type (upper panels) and *phyl*²³⁶⁶ mutant (lower panels) clones (green) were generated by the MARCM system, and examined at the indicated time points (days) ACI. Nuclei were stained with DAPI (blue).

(C) GFP marked *phyl*²²⁴⁵ mutant clones at 7 days ACI.

(D-E) Clones co-stained with PH3 to identify mitotic cells. (C) PH3⁺ cells could be detected in some wild-type *FRT42D* clones (yellow arrowhead). (D) PH3⁺ cells could not be detected in *phyl*²³⁶⁶ mutant clones.

Scale bar in A: 50 μ m, in C: 20 μ m.

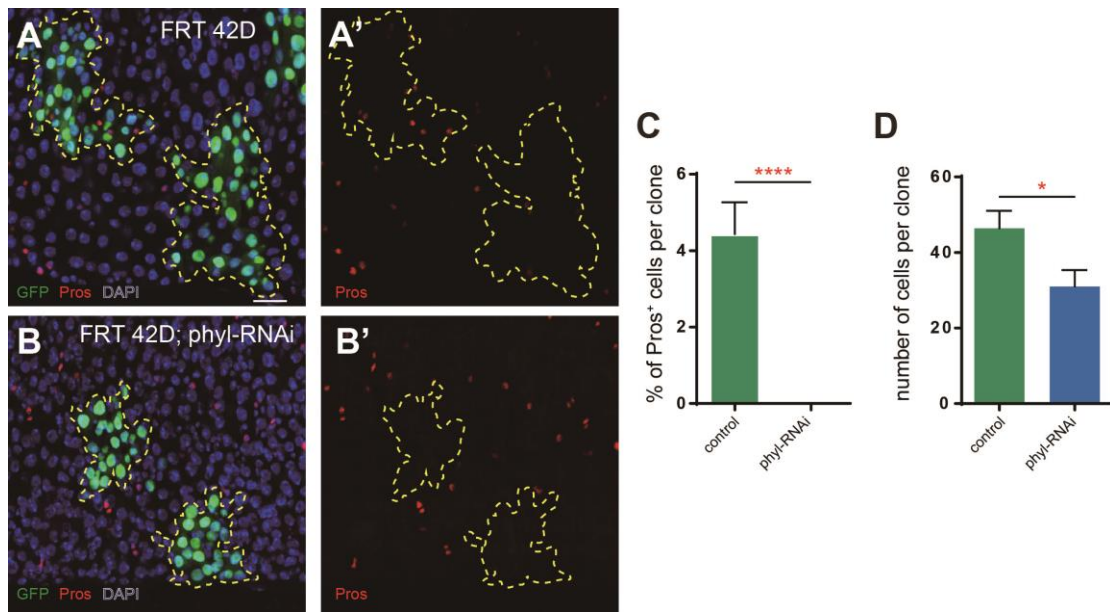


Fig. S3, Related to Figure 1. Effects of *phyl-RNAi* on ISC proliferation and EE differentiation.

Wild-type and *phyl-RNAi* homozygous clones (GFP, green) were generated by the MARCM system and were examined on 10 day after clone induction (ACI).

Clones were stained with anti-Pros (red). Note the absence of Pros⁺ cells in *phyl-RNAi* clones (dashed lines and separated channels).

The proportion of Pros⁺ cells per clone in wild-type and *phyl-RNAi* clones on days 10-14 ACI. Mean \pm s.e.m. $n=24$ for *FRT 42D* clones, $n=49$ for *phyl-RNAi* clones. **** $P<0.0001$ (Student's *t*-test).

Quantification of clone size of wild-type and *phyl-RNAi* clones on days 10-14 ACI. Mean \pm s.e.m. $n=24$ for *FRT 42D* clones, $n=49$ for *phyl-RNAi* clones. * $P<0.05$ (Student's *t*-test).

Nuclei were stained with DAPI (blue). Scale bar: 20 μ m.

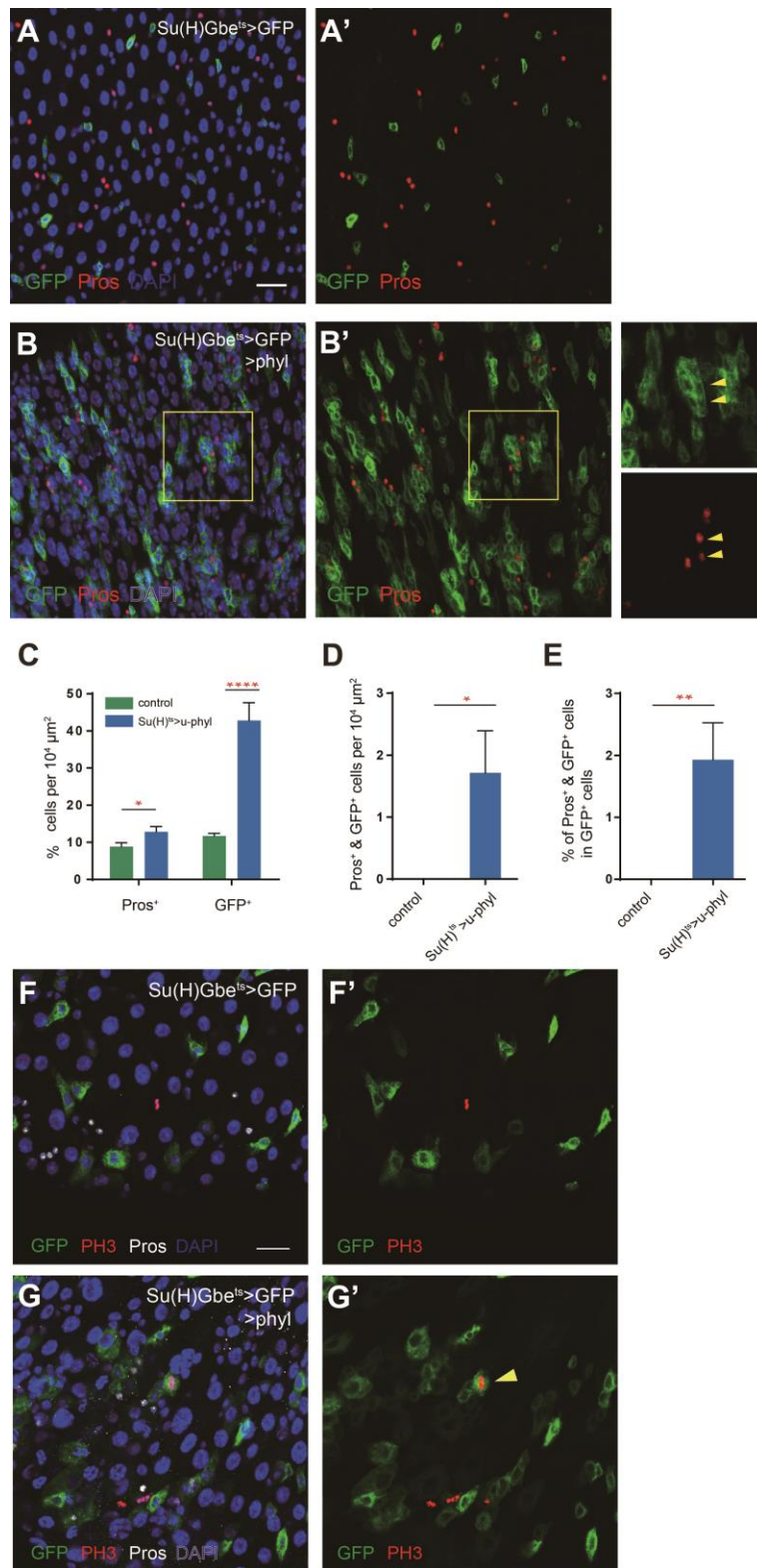


Fig. S4, Related to Figure 2. Overexpression of *phyl* in EBs causes EB accumulation and EE fate switch.

(A-B) Midgut epithelia of indicated genotypes stained with anti-Pros (red). Flies were shifted to the restrictive temperature for 14 days before analysis. Genotypes: *Su(H)Gbe-GAL4^{ts}, UAS-GFP* (A); *Su(H)Gbe-GAL4^{ts}, UAS-GFP; UAS-phyl* (B). GFP, green. Note that *phyl* overexpression causes increased number of EBs (GFP⁺), and some of these EBs adopt EE fate (GFP⁺ and Pros⁺).

(C) Quantification of the percentage of Pros⁺ or GFP⁺ cells per epithelial area in the intestines of indicated genotypes.

(D) Quantification of the total number of Pros and GFP double-positive cells per epithelial area.

(E) Quantification of the percentage of Pros and GFP double-positive cells in GFP positive cells.

Mean \pm s.e.m. $n=7$ (fields) for *Su(H)Gbe^{ts}>GFP*; $n=7$ for *Su(H)Gbe^{ts} >UAS-phyl* midguts in C-E. * $P<0.05$, ** $P<0.01$, **** $P<0.0001$ (Student's *t*-test).

(F-G) Mitotic cells, as indicated by PH3 staining (red, yellow arrowhead), were not present in *Su(H)Gbe^{ts}>GFP* cells in wild-type midgut (F). Overexpression of *phyl* driven by *Su(H)Gbe^{ts}* induced some *Su(H)Gbe>GFP* cells to re-enter mitosis (G).

Scale bars: 20 μ m.

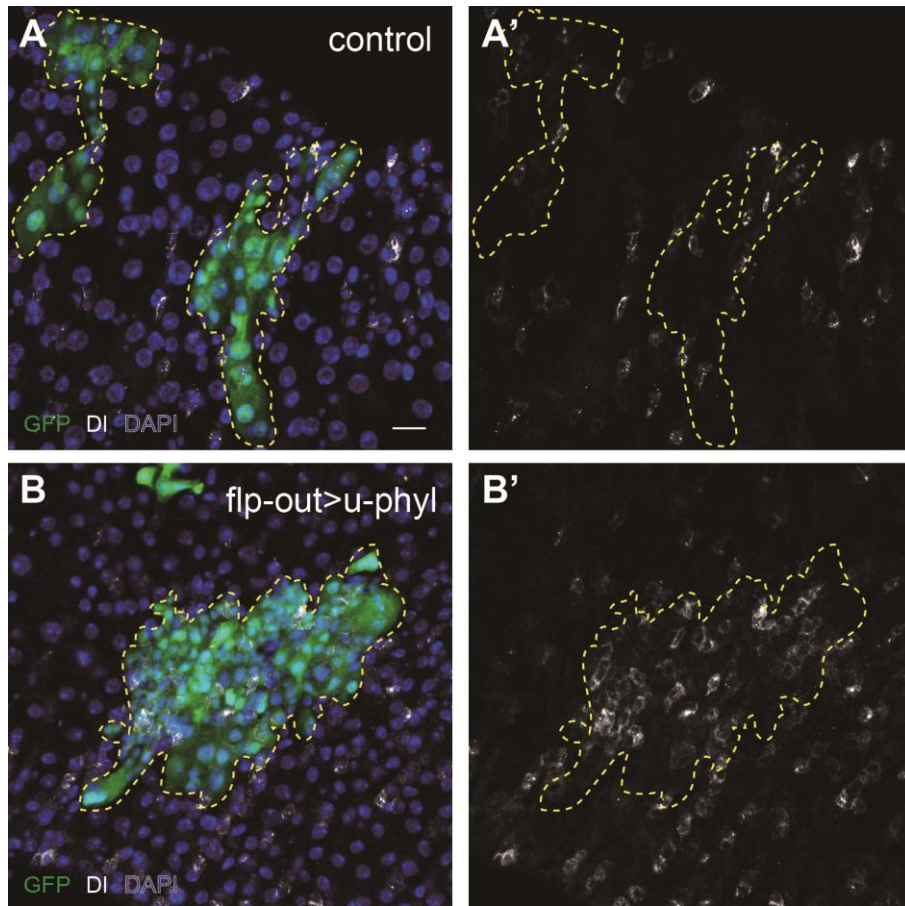


Fig. S5, Related to Figure 2. *phyl*-overexpressed clones contain extra ISC-like cells.

(A-B) Wild-type and *phyl* overexpression clones were generated by the flp-out system and were examined on 7 day ACI. Clones co-stained with anti-DI (white). Dashed lines depict the clone margin.

Scale bar: 20 μ m.

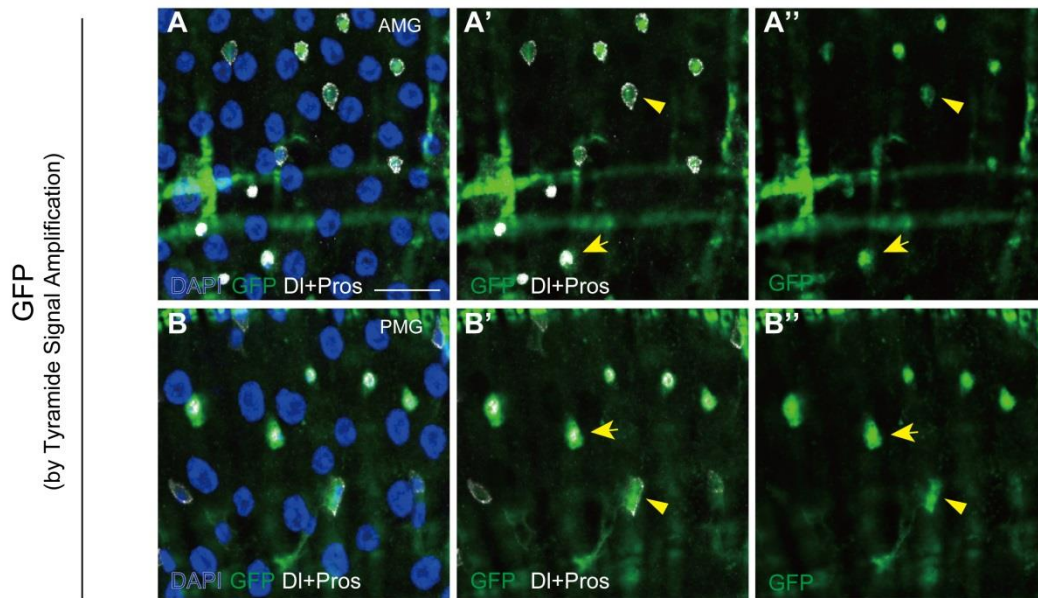


Fig. S6, Related to Figure 5. *phyl3.4-nGFP* expression pattern detected by the TSA method.

(A-B) The Tyramide Signal Amplification (TSA) method was used to amplify the GFP signal in *phyl^{3.4}-nGFP* intestines. With this method, GFP signal was detected in the majority of Pros⁺ EE s (yellow arrow) and DI⁺ ISCs (yellow arrowhead) at both the anterior (A) and the posterior (B) midgut regions.

Scale bar: 20 μ m.

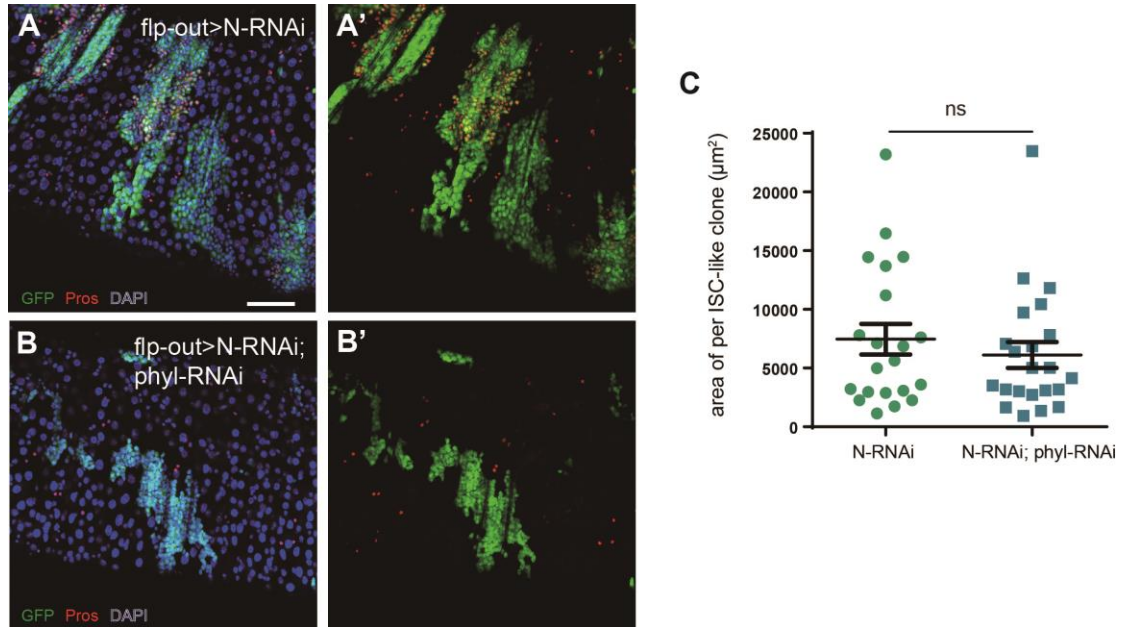


Fig. S7, Related to Figure 6. Depletion of *phyl* blocks *Notch*-loss-induced EE-like tumor formation.

(A-B) *N*-RNAi and *phyl*, *N* double RNAi clones were generated by the flp-out system and were examined on 14 day ACI. Clones co-stained with anti-Pros (red). Dashed lines depict the clone margin. Note the absence of EE-like tumors in *phyl*, *N* double RNAi clones, while ISC-like tumors still could be formed.

(C) Quantification of ISC-like tumor size in *N*-RNAi and *phyl*, *N* double RNAi clones. Mean \pm s.e.m. $n=21$ for *N*-RNAi clones, and $n=22$ for *phyl*, *N* double RNAi clones. ns, no significant difference.

Scale bar: 20 μ m.